Journal of Molecular Structure 1199 (2020) 127036

Contents lists available at ScienceDirect

Journal of Molecular Structure

journal homepage: http://www.elsevier.com/locate/molstruc

Synthesis, crystal structure, antioxidant activity and dft study of 2-aryl-2,3-dihydro-4H-[1,3]thiazino[3,2-*a*]benzimidazol-4-One

Omar Alejandro Ramos Rodríguez [a], Nancy Evelyn Magaña Vergara [a], Juan Pablo Mojica Sánchez [a, b], María Teresa Sumaya Martínez [c], Zeferino Gómez Sandoval [a], Alejandro Cruz [d], Ángel Ramos Organillo [a, *]

[a] *Facultad de Ciencias Químicas, Universidad de Colima, Km 9 Carretera Colima-Coquimatlán, Coquimatlán, Colima, C.P. 28400, Mexico*
[b] *Instituto Tecnológico José Mario Molina Pasquel y Henríquez Campus Tamazula de Gordiano, Carretera Tamazula-Santa Rosa, Tamazula de Gordiano, Jalisco, No. 329, C.P. 49650, Mexico*
[c] *Unidad de Tecnología de Alimentos. Universidad Autónoma de Nayarit, Cd. de la Cultura "Amado Nervo", Boulevard Tepic-Xalisco s/n, Tepic, Nayarit, C.P. 63190, Mexico*
[d] *Laboratorio de Química Supramolecular y Nanociencias Instituto Politécnico Nacional-UPIBI, Av. Acueducto s/n, Barrio La Laguna Ticomán, Ciudad de México, C.P. 07340, Mexico*

ARTICLE INFO

Article history:
Received 12 April 2019
Received in revised form
3 September 2019
Accepted 4 September 2019
Available online 7 September 2019

Keywords:
Thiazine ring
Crystal structure
Hydrogen bonding
DFT
Hirshfeld surface
Antioxidant activity

ABSTRACT

The compound 2-aryl-2,3-dihydro-4H- [1,3]thiazino[3,2-*a*]benzimidazol-4-one ($C_{16}H_{12}N_2OS$) (**III**) was synthesized. The compound crystallized in a monoclinic crystal system with $P2_1/c$ space group as revealed by mono-crystal X-ray diffraction. The X-ray analysis and density functional theory complementary calculations showed that noncovalent C—H···π interactions between the benzimidazole system and the thiazine ring form a dimerization along the direction of the *b* axes, additionally π···π interactions were found between the benzene rings. The C12, in the thiazine ring, has a distortion angle (41.69°) respect to the plane of benzimidazole. The intermolecular interactions in the crystal structure were quantified and analyzed using Hirshfeld surface analysis. The predominant interaction within the crystalline structure was found to be H···H interaction. On the other hand, antioxidant activity of the $C_{16}H_{12}N_2OS$ system was studied using the DPPH• and $ABTS^{•+}$ assay. Using the energy profile for the reaction of DPPH• with **III** it was demonstrated that the antioxidant activity is carried out through HAT (H12) mechanism where conjugation of the radical can occur between the C12 of the thiazine ring and the aromatic ring, this was confirmed by a H function calculation. The importance of this study focuses on the promising range of biological activities and molecular characteristics of the synthesized compound (**III**).

1. Introduction

Benzimidazole has acidic and basic characteristics (pKa 2.5). The —NH— group present in the imidazole ring is relatively acid, while pyridine-type nitrogen is basic. In benzimidazoles —NH— presents prototropic tautomerism. But when the group attached to the nitrogen atom is larger than hydrogen, tautomerization is not well defined [1].

1H-Benzimidazole-2(3H)-thione and its derivatives have different applications in several areas such as pharmacology and industry [2]. The main biological activities are: progesterone antagonist, antinematode activity, while 2-(alkylithium)-benzimidazole with ring β-lactamics presents antibacterial and antifungal activity. In addition, it has been found that structural modifications of the lateral chain and stereochemistry results in substantial improvements in *anti*-HIV potency [3], cancer and virus [4].

Thiazine is a six membered ring that contains nitrogen and Sulphur heteroatoms at positions 1 and 3. Previously it was proposed by Britsun & Lozinskii [5] that thiazine ring synthesis is a sequence of at least two successive reactions. Thiazines are very useful compounds in medicinal chemistry and have been reported to exhibit a wide variety of biological activities such as

* Corresponding author.
E-mail addresses: aaramos@ucol.mx, aa.ramos.o@gmail.com (Á. Ramos Organillo).

https://doi.org/10.1016/j.molstruc.2019.127036
0022-2860/

antimicrobials [6,7], antivirals [8], antifungals [9], antihistamine [10] and antioxidant [11]. Derivatives of 4H-1,3-thiazin-4-one have biological activity and are used as pesticides, herbicides, fungicides and antituberculosis agents. The compound 2-aryl-2,3-dihydro-4H- [1,3]thiazino [3,2-a]benzimidazole-4-one under this study and its crystal was obtained from a different methodology compared to the one reported by Britsun & Lozinskii [5], to improve the reaction yield, explore the molecular structure, and determine its antioxidant activity, since it has been described above that this type of compound presents analgesic, anticonvulsant, antianxiolytic and antioxidant activity [12].

The importance of antioxidant activity in these compounds lies in the fact that they offer protection in internal and external oxidation processes, which results in an excess of reactive molecules that cause cellular aging, cardiovascular alterations and cancer [13]. The possible antioxidant activity lies in the structural characteristic of the system. The presence of thiazine ring allows conjugation, and the sulphur atom stabilizes the charge. In recent years, a wide range of spectrophotometric assays has been adopted to measure antioxidant capacity of foods and compounds, the most popular being 2,20-azino-bis-3-ethylbenzthiazoline-6-sulphonic acid (ABTS) and 1,1-diphenyl-2-picrylhydrazyl (DPPH) assay. The difference between DPPH and ABTS is that the ABTS assay is applied to a variety of hydrophilic, lipophilic and highly pigmented antioxidant compounds [14].

In recent years, a wide range of spectrophotometric assays have been adopted to measure the antioxidant capacity of foods and compounds, the most popular being 2,20-azino-bis-3-ethylbenzothiazolin-6-sulfonic acid (ABTS) and the 1,1-diphenyl-2-picrylhydrazil assay (DPPH). The difference between DPPH and ABTS is that the ABTS assay applies to a variety of hydrophilic, lipophilic, and highly pigmented antioxidant compounds [14].

On the other hand, the dizzying development of computation has allowed theoretical and computational chemistry to flourish. Under this approach different methodologies have been developed, such as the density functional theory, which has permitted the study of chemical systems. One of the problems that has attacked the theory has been the explanation of the non-classical interactions, specifically with the non-covalent index [15], besides in solid state the use of Hirshfeld surfaces allows to know the inter and intramolecular contacts of a crystal [16,17]. Another application includes the study of chemical reactions, predicting the most favored reaction mechanisms and the study of the transition state, being key in the study of antioxidant capacity.

Here we report the crystalline structure of the compound 2-aryl-2,3-dihydro4H- [1,3]thiazino [3,2-a]benzimidazole-4-ones, and its antioxidant activity by experimental and theoretical calculations, in the search for new compounds with high anti-radical activity.

2. Experimental

2.1. Material and methods

All reagents (Cinnamic acid, 2-mercaptobenzimidazole, 4-Dimethylaminopyridine (DMAP) and N,N′-Dicyclohexylcarbodiimide (DCC)) were purchased from Sigma Aldrich and used as received. The solvents used were dried before use by standard techniques [18]. Analysis of ^{1}H and ^{13}C NMR spectra of compound III was carried out in $CDCl_3$ as solvent and tetramethyl silane (TMS) as internal reference, were recorded using Bruker Ultrashield Plus 400 (1H, 400; 13C, 100.62 MHz) instrument. Melting point was measured in a Melt-Temp equipment. The most characteristic functional groups present in the synthesized molecule were identified using a Varian 3100 FT-IR spectrometer of the Excalibur series in the range 4000−600 cm^{-1}. The elemental analysis was performed on a Leco TruSpect Micro (C, H, N) analyzer under standard conditions.

2.1.1. Synthetic procedure 2-aryl-2,3-dihydro-4H- [1,3]thiazino [3,2-a]benzimidazol-4-one (III)

The compound (**III**), Scheme 1, was obtained by mixing *trans*-cinnamic (**II**) acid (1.00 g, 6.7 mmol) with 2-mercaptobenzimidazole (**I**) (1.01 g, 6.7 mmol) and 4-(Dimethylamino)pyridine (DMAP) in catalytic amounts (10%) (0.08 g, 0.67 mmol) in 30 mL of dry CH_2Cl_2, followed by the slow addition of N,N′-Dicyclohexylcarbodiimide (DCC) (1.39 g, 6.7 mmol) in 10 mL of dry CH_2Cl_2. The reaction mixture was kept in an ice bath with continue stirring for 1 h, then left at room temperature and constant stirring overnight. Dicyclohexylurea (DCU) was filtered off and the solvent was removed by evaporation at reduced pressure. To the dry product 30 mL ethyl acetate was added to perform two acid washes with HCl (0.05 N) solution, two basic washes with a 5% solution of K_2CO_3, and two washes with distilled water. The ethyl acetate was then dried out with anhydrous magnesium sulphate and filtered, the solvent was removed by evaporation at reduced pressure to get the compound.

The resulting compound (**III**) was a yellow solid crystallizing in a mixture of dichloromethane-hexane solvents (3:7); (yield 76%, 1.428 g; **m. p.** 121−122 °C). **IR** (KBr, ν_{max}, cm^{-1}): 1720.49 (C═O), 1473 (N−C−S), 1451.19 (C−N), 694.52 (C−S); **^{1}H NMR** ($CDCl_3$): δ 8.17 (1H, m, H5), 7.63−7.33 (8H, m, Ar), δ ABX 5.41 (1H, m, H12), 3.84 (1H, m, H11), 3.40 (1H, m, H11); **^{13}C NMR:** δ 167.2 (C10), 151.1 (C2), 142.8 (C8), 137.4 (C13), 132.3 (C9), 129.3 (C15, C17), 128.9 (C14, C18), 127.6 (C5), 125.4 (C6), 124.4 (C4), 118.5 (C7), 42.6 (C12), 41.3 (C11). Elemental analysis calculated for $C_{16}H_{12}N_2OS$: C 68.55, H 4.31, N 9.99%; found: C 68.57, H 4.47, N 9.95%.

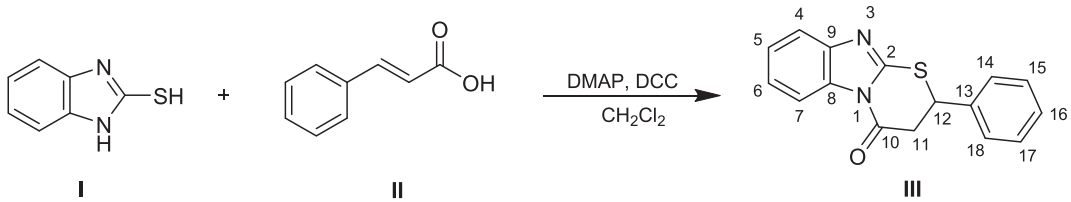

DMAP= 4-(dimethylaminopyridine)
DCC= N,N-Dicyclohexylcarbodiimide

Scheme 1. Schematic representation of the synthesis of (**III**).

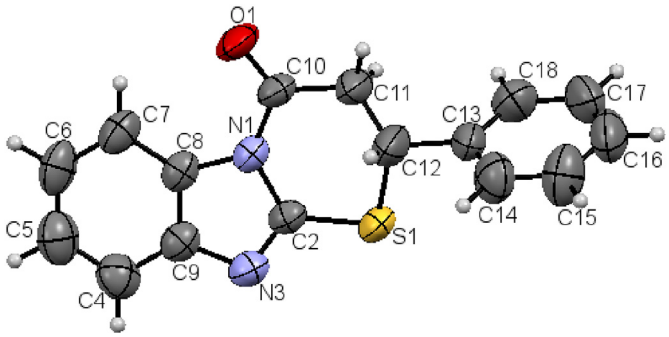

Fig. 1. Molecular structure of compound (**III**) showing the atom-numbering scheme. Displacement ellipsoids are drawn at the 50% probability level.

2.2. X-ray structure elucidation

The single crystal X–ray diffraction data was collected on a Bruker AXS D8 QUEST with Mo Kα (λ = 0.73 Å) radiation at 293 K. The cell refinement and data reduction were carried out with the SAINT V8.34A (Bruker, Madison, WI, USA) [14], WinGX [19] software. The structure was solved by direct methods using SHELXL97 (University of Göttingen, Germany) [20]. H atoms on C and N were positioned geometrically and treated as riding atoms, with CH = 0.95−0.99 Å and Uiso(H) = 1.5 Ueq(C) for methyl H atoms or 1.2Ueq(C) otherwise, and N−H = 0.88 Å and Uiso(H) = 1.2Ueq(N). Mercury software (The Cambridge Crystallographic Data Centre, Cambridge, UK) [21] was used to prepare the material for publication. CCDC 1908882 contains the supplementary crystallographic data for this paper. These data can be obtained free of charge via http://www.ccdc.cam.ac.uk/conts/retrieving.html (or from the Cambridge Crystallographic Data Centre, 12, Union Road, Cambridge CB2 1EZ, UK; fax: +44 1223 336033).

2.3. Antioxidant activity

The synthesized compound **III** was screened for their antioxidant activity by 1,1-diphenyl-2-picrylhydrazyl (DPPH•) radical scavenging assay and 2,2-azinobis (3-ethyl benzothiazoline-6-sulfonic acid) $ABTS^{\bullet+}$ radical cation decolorization method.

A Power wave XS microplates reader from biotek were used to read the absorbencies. Micropipettes (Thermofisher 89 finnpipette) of different capacities (25, 200, 1000 μL) were also used to prepare the required solutions. Eppendorf tubes (1 mL) were used for sample preparation. All tests were carried out in triplicate. For each run of samples a standard curve was made using the reference antioxidant in order to calculate the equivalents per mL of the reference antioxidant [22].

2.3.1. DPPH• method

A solution of DPPH• (7.4 mg/100 mL) was prepared and kept in the dark to avoid photodegradation. 50 μL were taken from a DMSO solution of compound **III** or the reference antioxidant (Trolox) to which 250 μL of DPPH• solution was immediately added. The mixture was stirred vigorously with a microvortex and left it to stand at room temperature for 1 h, then the absorbance was measured at 520 nm. The results of anti-radical activity were expressed as a percentage of inhibition and on μmol trolox/L equivalents (μmol TE/L) [23–26].

2.3.2. $ABTS^{\bullet+}$ method

The radical $ABTS^{\bullet+}$ was obtained by reacting $NH_4^+ABTS^{2-}$ (7 mM) with potassium persulphate (2.45 mM) for 16 h at 4 °C in the dark. Once formed, the radical $ABTS^{\bullet+}$ was diluted with ethanol to obtain absorbance value of 0.70 (±0.1) at 754 nm. In an eppendorf tube 490 μL of the diluted solution of free radicals ($ABTS^{\bullet+}$) and 10 μL of the compounds to be analyzed or vitamin C (reference antioxidant) were added, the mixture was agitated vigorously and then 200 μL of this mixture were taken and its absorbance was read at 754 nm in a microplates reader. The results of anti-radical activity were expressed as a percentage of inhibition and in milligrams ascorbic acid equivalents per liter (mg AAE/L) [23–26].

2.4. Computational methods

The computational calculations were performed using the density functional theory framework as implemented in the Gaussian 09 program [27]. For the exchange and correlation functional, the hybrid functional B3LYP was used [28]. The 6-311G(d,p) basis set was employed for the atomic species [29]. The non-covalent interaction index was calculated from the electron density in the Multiwfn package [30] and the relation were plotted using the VMD program [31]. For to determine the transition state of DPPH• molecule, considering all possible sites of dehydrogenation, the intrinsic reaction coordinate was utilized. In addition, the SMD model was included considering the effects of the DMSO solvent and the Grimme's correction with Becke-Johnson damping was considered account to include the dispersion [32].

Analysis of Hirshfeld surfaces and 2D fingerprints were obtained

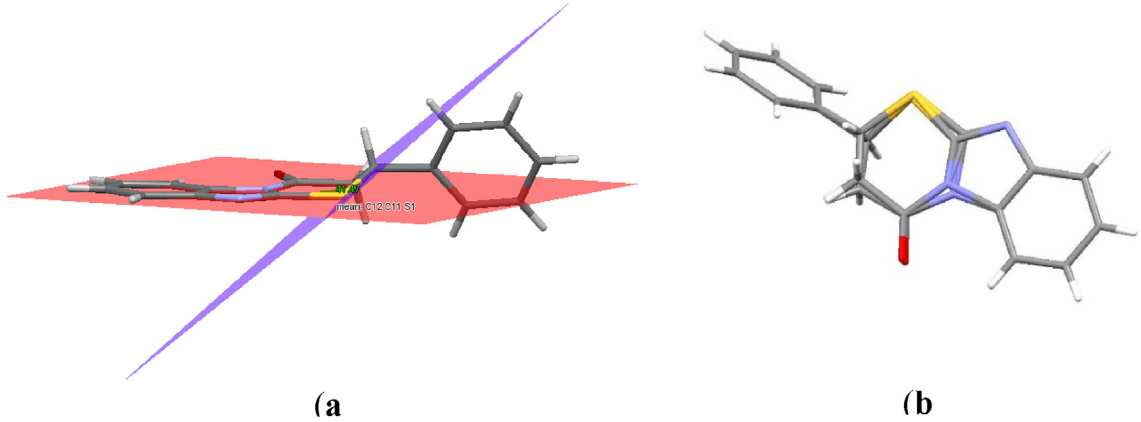

Fig. 2. Compound (**III**) planes, (**a**) where (C12) of the thiazine ring has angular tension and (**b**) heterocyclic ring thiazine disordered over two positions with a 50:50 occupancy caused by ring disorder.

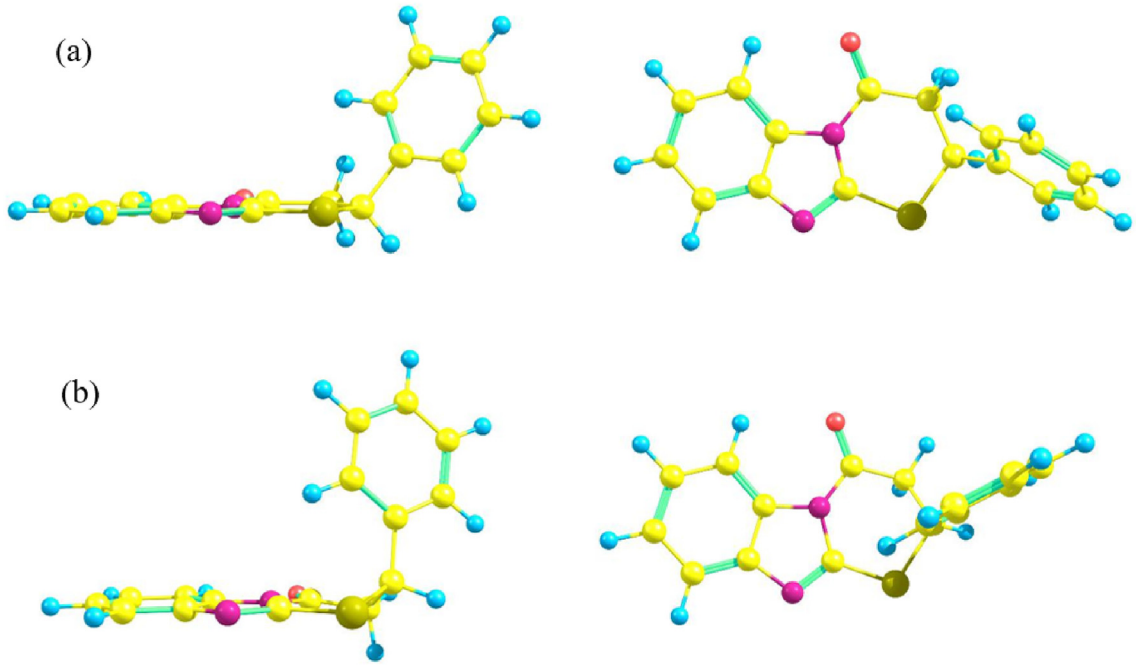

Fig. 3. Conformations of compound III. In this figure two conformers are shown. In figure (**a**) shows the thiazine ring presents torsional tension, remaining in the same plane as the benzimidazole. In (**b**) shows a lower potential energy since the carbon of the thiazine that binds to the phenyl leaves the plane of the benzimidazole decreasing the torsional tension.

Table 1
Hydrogen-bond geometry (Å, °) for (**III**).

D—H···*A*	*D*—H	H—*A*	*D*—*A*	*D*—H—*A*
C7—H7···O1	0.95	2.48	2.971 (7)	112
C4—H4···N3^{i}	0.95	2.57	3.478 (8)	160
C12—H12···O1^{ii}	1	2.44	3.293 (8)	143

Symmetry codes: (i) −*x*+1, −*y*, −*z*+1; (ii) −*x*+1, *y*−1/2, −*z*+3/2.

in Crystal Explorer 3.1 [33]. The graphs of Hirshfeld's molecular surfaces were mapped with d_{norm} using a scheme colors, where the red one represents the shortest contacts, the white color indicates intermolecular distances close to the van der Waals contacts with d_{norm} equal to zero, and the blue color shows the contacts longer than the sum of the van der Waals radii with positive d_{norm} values [34].

3. Results and discussion

3.1. Synthesis

Experimental data from NMR, IR, elemental analysis and crystal X-ray diffraction give information that confirms the synthesis of compound **III**. 2-Mercaptobenzimidazole exists as a mixture of thione and thiol forms, where heterocyclization certainly proceeds through the thiol form. Experimentally, the reaction is a one-step process, although it has been proposed that it is a sequence of at least two successive reactions, where N-acylation and the addition of the mercapto group to the double bond occur [5].

In the ^{1}H spectrum at NMR of compound **III**, the protons H11A, H11B and H12 show an ABX coupling system. The ABX spectra is produced by a special type of three-spin system in which two non-equivalent nuclei are strongly coupled and each of them is weakly coupled to a third non-equivalent nuclei. In the spectrum of 1H (between 5.50 and 3.30 ppm) the three quadruple signals correspond to these non-equivalent protons. Peaks corresponding to aromatic protons were appeared between 7.33 and 8.17 ppm.

The ^{13}C NMR spectra show signals according to the structure of compound **III**. The carbonyl signal (C10 = O) of the amidic group is presented at 167.2 ppm, while aromatic carbon peaks occur between 118.5 and 151.1 ppm [5]. These variations are due to the chemical environment and functional groups found near these nuclei.

3.2. X-ray diffraction of compound III

Suitable crystals for compound **III** were obtained from saturated solution by slow evaporation of the solvent at room temperature. The compound **III** crystallized in the monoclinic space group $P2_1/c$, Fig. 1. The dimensions of the cell are as follows: a = 13.543 (1), b = 5.827 (4), c = 18.022 (14) Å, V = 1358.97 Å^3 with four units per asymmetric unit (Z = 4). The molecular structure was drawn with 50% probability level displacement ellipsoids, together with the atomic numbering scheme is exhibited in Fig. 1. The anisotropic refinement also showed the heterocyclic ring thiazine disordered over two positions with a 50:50 occupancy (Fig. 2b), as is commonly observed in flexible fragments containing cycloalkanes functionalities. The angle between C2—S1—C12 of the thiazine ring is 99.5°; the angle formed in S1—C2—N1 is 122.9° and that of C2—N1—C10 is 127.9°. The distance S—C is 1.731 (C2—S1) and 1.798 (C12—S1) Å.

The thiazine ring is formed by 6 members that have an angular tension in the carbon (C12) of 41.47° with respect to the plane formed by the benzimidazole (Fig. 2), this angular tension produces a decrease of the torsional tension so that the net result is a decrease of the global energy), being this conformation 14.746 kcal/mol more stable (Fig. 3).

Crystal data, data collection and structure refinement details are summarized in Supplementary Material Table S1. The compound (**III**) presents three non-covalent intra-molecular interactions with

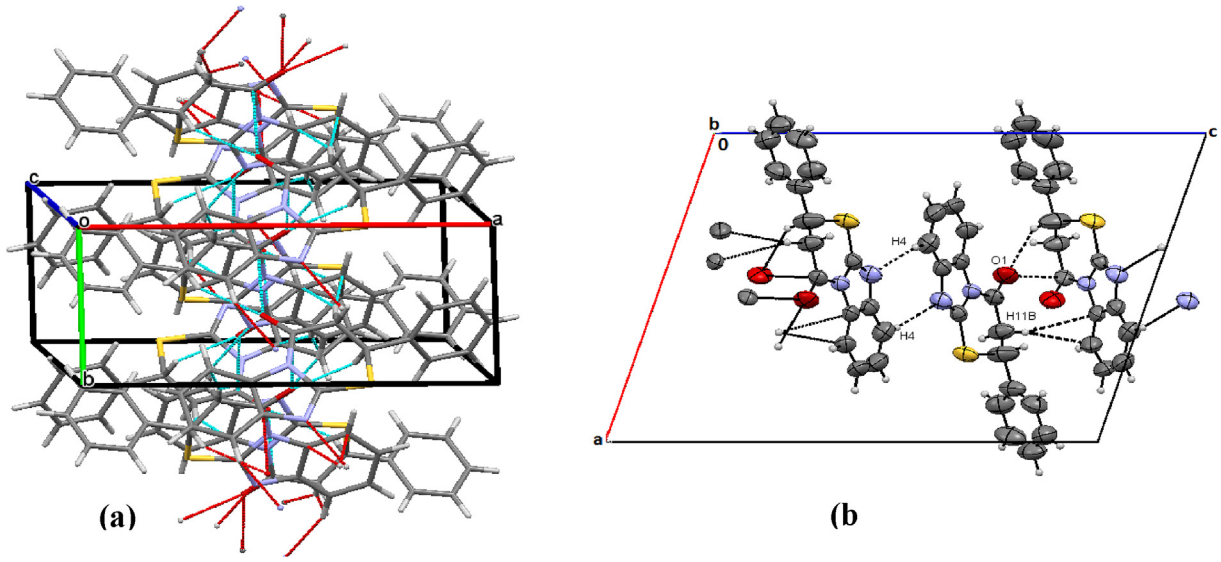

Fig. 4. **(a)** The crystal packing diagram of (**III**) along the direction of the *b* plane. **(b)** A detailed view of the formation of the hydrogen-bonding motif and the π—π stacking interactions.

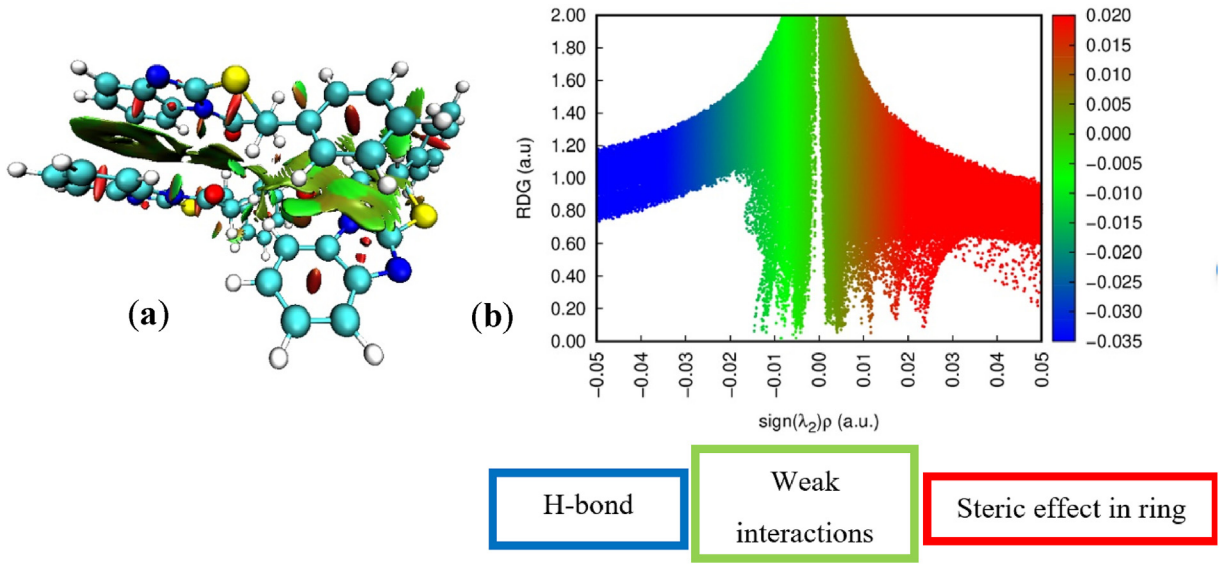

Fig. 5. (**a**) Noncovalent interactions analysis of the 2-aryl-2,3-dihydro-4H- [1,3]thiazino [3,2-a]benzimidazol-4-one and (**b**) reduced density gradient (RDG) graph. The surfaces are colored according to sign(λ_2)ρ over the range −0.05 to 0.05 a.u.

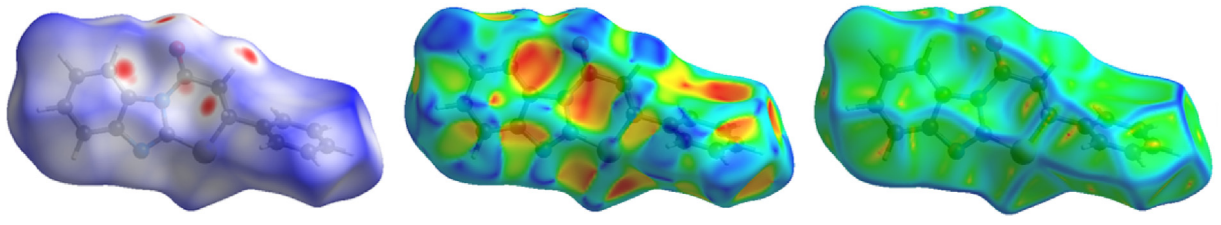

Fig. 6. Hirshfeld surface, shape index, and curvedness for the crystal structure.

codes of symmetry that can be seen in Table 1. With distances and angles C4···N3 of 3.478 Å (159.72°); C12···O1 of 3.293 Å (143.40°); C11···C7 of 3.638 Å (168.23°) and C11···C8 of 3.718 Å (153.88°) where C11 presents itself as a bifurcated donor (Fig. 4b). In addition, interactions π···π between the imidazole and benzene rings are observed in the dimerization of the compound and extends along *b* plane (Fig. 4a).

The compound (**III**) presents an interesting structure, with

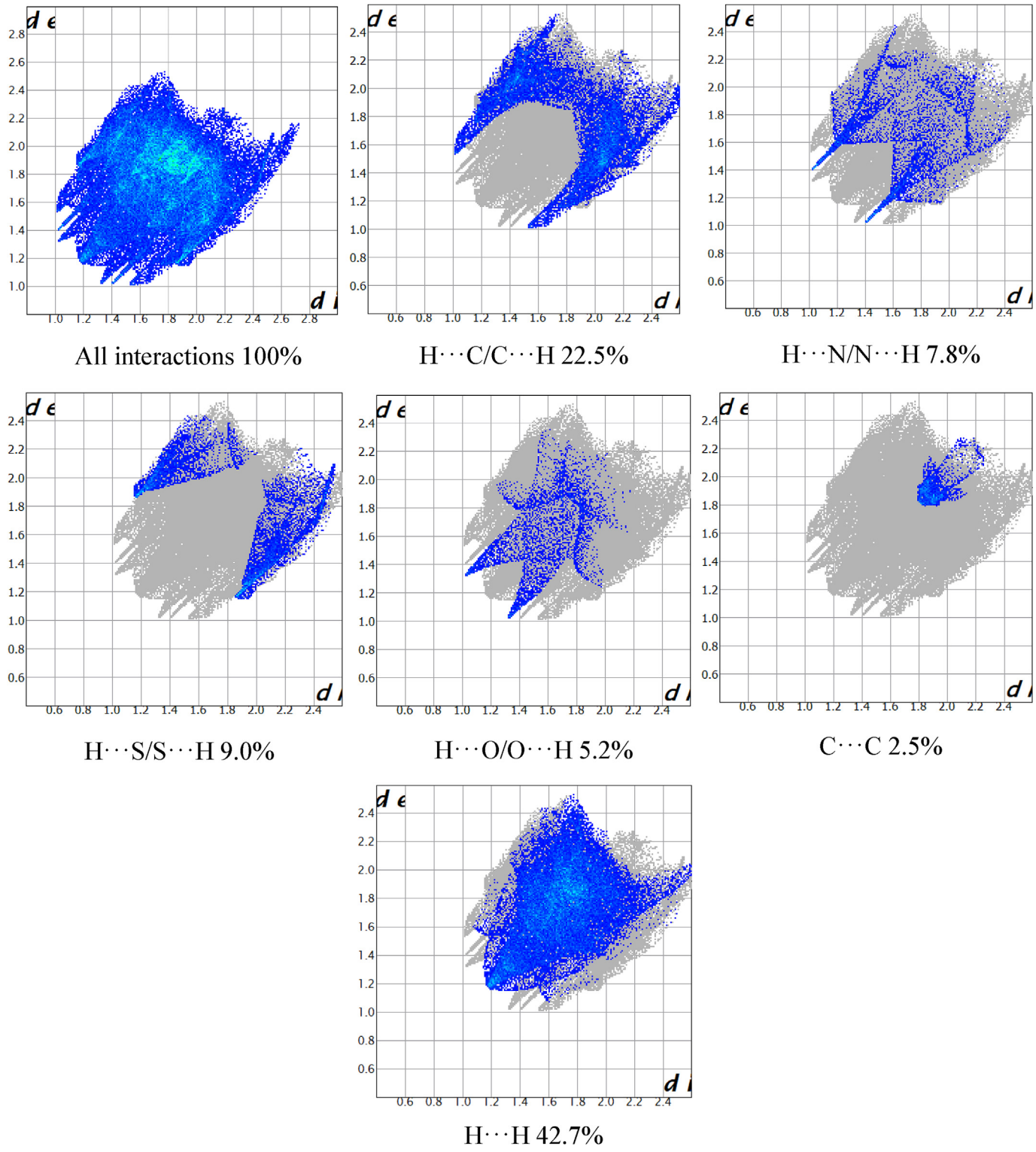

Fig. 7. Fingerprints plots of the total and specific intermolecular contacts of the crystal structure.

conformational properties in the thiazine ring. As can be seen in the structure of (**III**) the growth of the chain is given by non-classical interactions extending along *b* axis.

3.3. Non-covalent interactions and Hirshfeld surface analysis

The fundamental problem in the study of a crystal is to understand the role of strong and weak molecular interactions in the crystal packing. The noncovalent interaction (NCI) index is a successful tool to describe different type of interactions. In this context, the reduced density gradient is plotted, and the sign(λ_2) enables the identification of attractive or repulsive interactions [15]. Fig. 5 shows the plot of the NCI of 2-aril-2,3-dihidro-4H- [1,3] thiazino [3,2-a]benzimidazol-4-one. The strong attractive

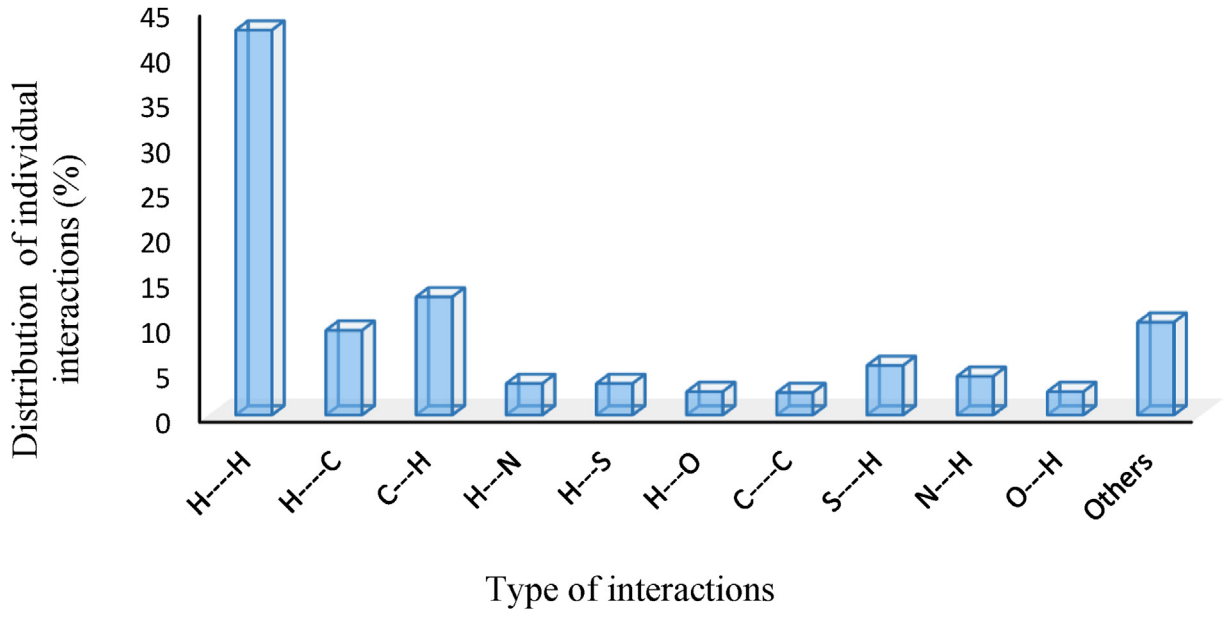

Fig. 8. Contribution of intermolecular contacts to the Hirshfeld surface of the crystal structure.

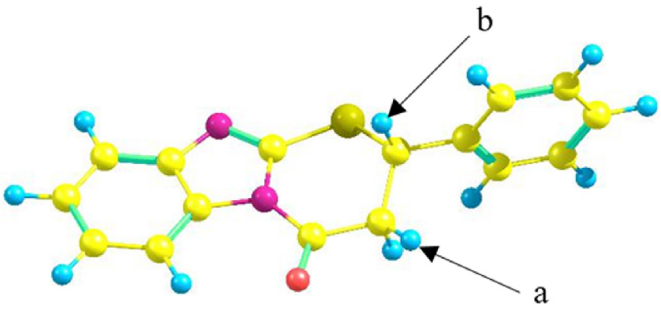

Fig. 9. Potential molecular sites (**a** and **b**) where hydrogen transfer may occur.

interaction is indicated in blue and the red color stands a strong repulsive interaction. Additionally, weak interactions are highlighted by a green isosurface.

In the Fig. 5 shows predominant green areas, which correspond a local intermolecular contact regions, specifically: 1) $\pi\cdots\pi$ interactions between the benzene rings, 2) $CH\cdots\pi$ interactions between the benzimidazole system and the thiazine ring. Furthermore, hydrogen-bonding and steric repulsion were also found. With greater notoriety, steric clashes were located in the benzene and the thiazine rings. Kitaigorodskii made one of the arguments of the balance between attractions and repulsions between molecules in a crystal, referring to key-and-lock mechanism, whereby the molecules tend to adapt a shape where the best packing is favored.

Another tool used to analyze molecular crystalline structures that has rapidly gained popularity is the Hirshfeld surface. In this technique a weight function can be defined for a molecule in a crystal. One of the most powerful applications of the Hirshfeld surface is the identification of molecular contacts. Fig. 6 presents the Hirshfeld surface, the shape index and the curvedness of the 2-aryl-2,3-dihydro-4H- [1,3]thiazino [3,2-a]benzimidazole-4-one. Mainly, shape index and curvedness identify characteristic packing modes, planar stacking arrangements and the way neighboring molecules contact each other. In the Fig. 6, the curvedness surfaces show broad and relatively flat regions, characteristic of planar stacking of molecules, over benzene and thiazine rings specifically.

The information of the Hirshfeld surface can translate in 2D plots called fingerprints. The Hirshfeld surface is mapped over the $d_{norm.}$ In the fingerprints d_e represents the distance from the point to the nearest nucleus external to the surface and d_i corresponds to the distance to the nearest nucleus internal to the surface [30]. The principal contacts in form of 2D fingerprints were interactions: H···H, H···C/C···H, H···N/N···H, H···S/S···H, H···O/O···H, C···C that are illustrated in Fig. 7 and their relative contributions to the Hirshfeld surface are depicted in Fig. 8.

The major contribution to the total Hirshfeld surfaces analysis was the H···H interactions (42.7%), which confirms the importance of this bond in the stability of a crystal [16]. Another majority contact was the H···C/C···H interaction (22.5%), that interaction appear as two spikes with the same $d_e + d_i \sim 2.6$ Å, the H···C/C···H contacts corresponds to $CH\cdots\pi$ interactions [17].

The C···C interactions presents in the Hirshfeld surfaces represents $\pi\cdots\pi$ stacking arrangements with values $d_e \approx d_i$ ~1.8 Å (Fig. 7). Concerning the H···N/N···H contacts values of $d_e + d_i$ ~2.4 Å was obtained and with respect to H···S/S···H interactions with a contribution of 9% is the responsible of the Hirshfeld surface of the crystal. Finally, another type of contacts contributes with only 10.3%.

3.4. Antioxidant activity

3.4.1. DPPH• method

The assay of DPPH• was carried out in triplicate and the inhibition percentage was calculated using the following formula.

$$\%\ \text{inhibition} = \frac{A_C - A_S}{A_C} \text{x } 100$$

where, A_C is absorbance of DPPH• alone, A_S is absorbance of DPPH• with the compound **III**.

The result of the antioxidant activity of the compound 2-aryl-2,3-dihydro-4H- [1,3]thiazino [3,2-a]benzimidazole-4-one (**III**) showed good values of % Inhibition (73% ± 2.42), which compared to the reference antioxidant trolox (70% ± 0.35) indicates a high antioxidant activity against DPPH• radical. In addition, compound

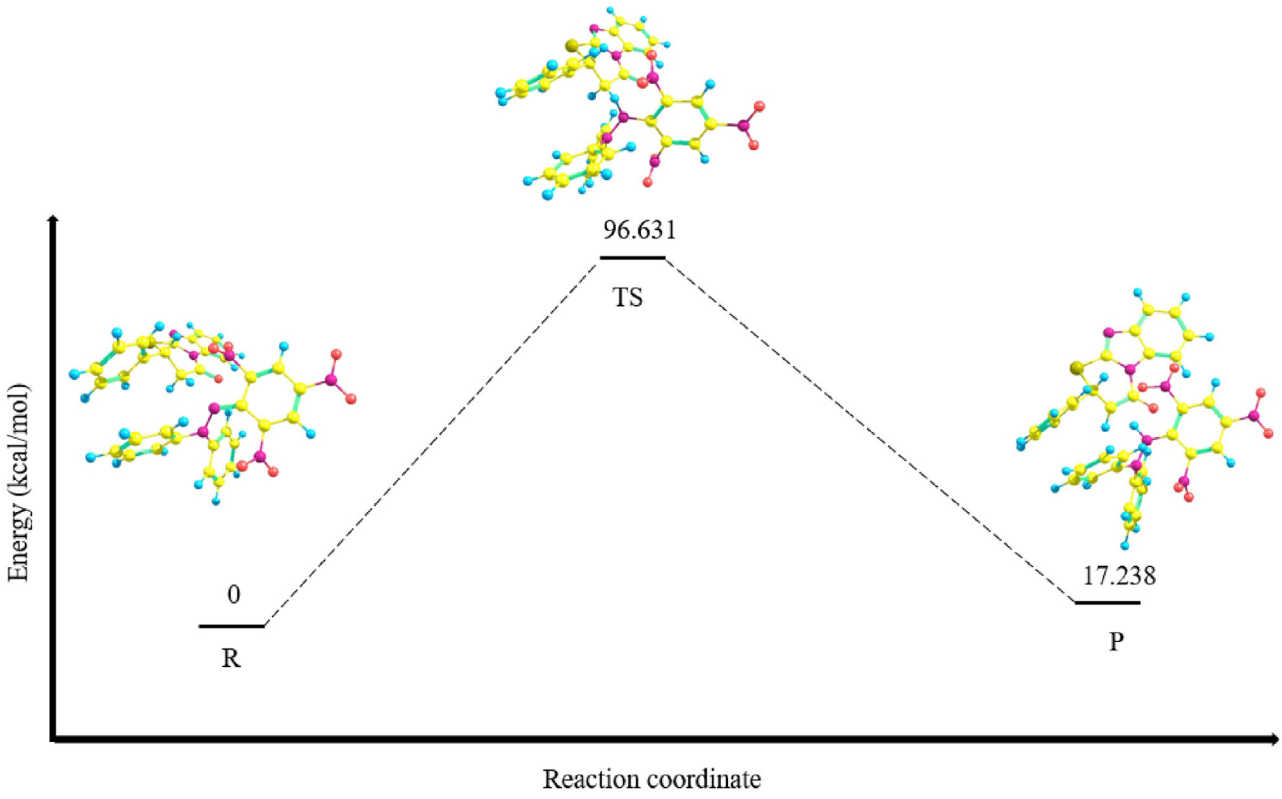

Fig. 10. Energy profile of the dehydrogenation reaction at DPPH• site **a**.

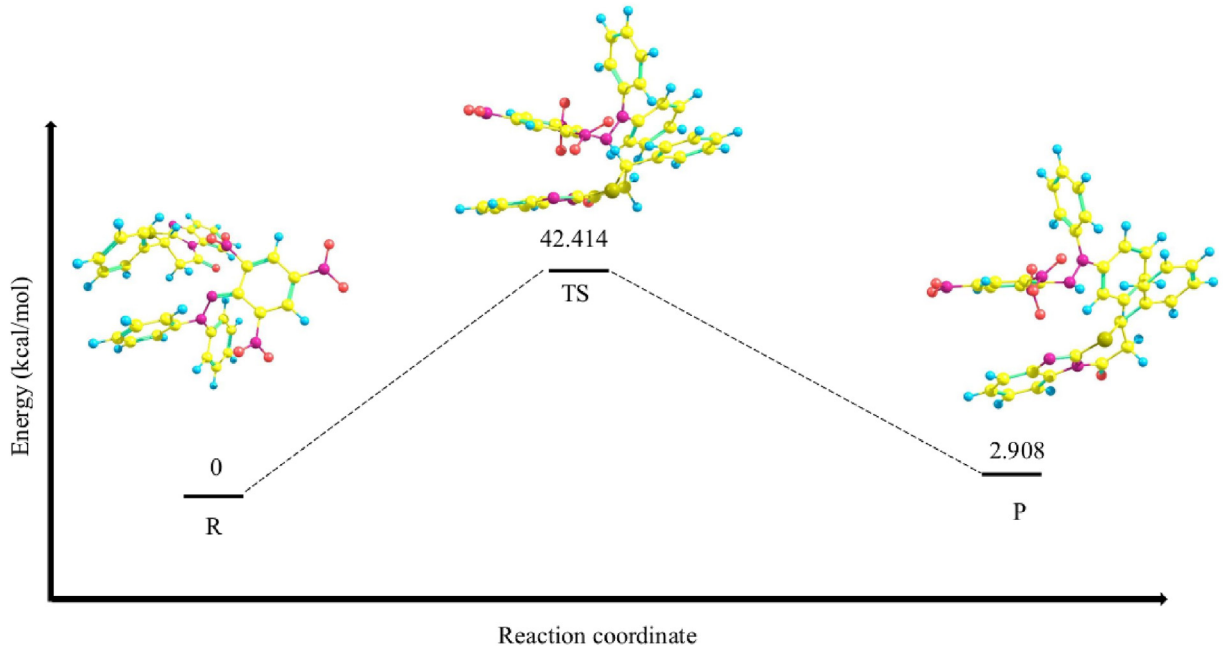

Fig. 11. Energy profile of the dehydrogenation reaction at DPPH• site **b**.

III presented a value of 291 ± 7.6 μMol TE/L confirming the high antioxidant activity.

The DPPH• radical can be reduced by two mechanisms: Hydrogen Atom Transfer (HAT) and Electron Transfer (ET) [35]. There are differences of opinion among researchers about the reduction mechanism of DPPH, some of them define it as a suitable radical for the ET measurement method, while other authors classify it for the HAT method. However, it is necessary to take into account the structural characteristics of the antioxidant used [36]. In this assay of antioxidant activity of compound **III**, the HAT mechanism can better explain the result obtained in inhibition DPPH•.

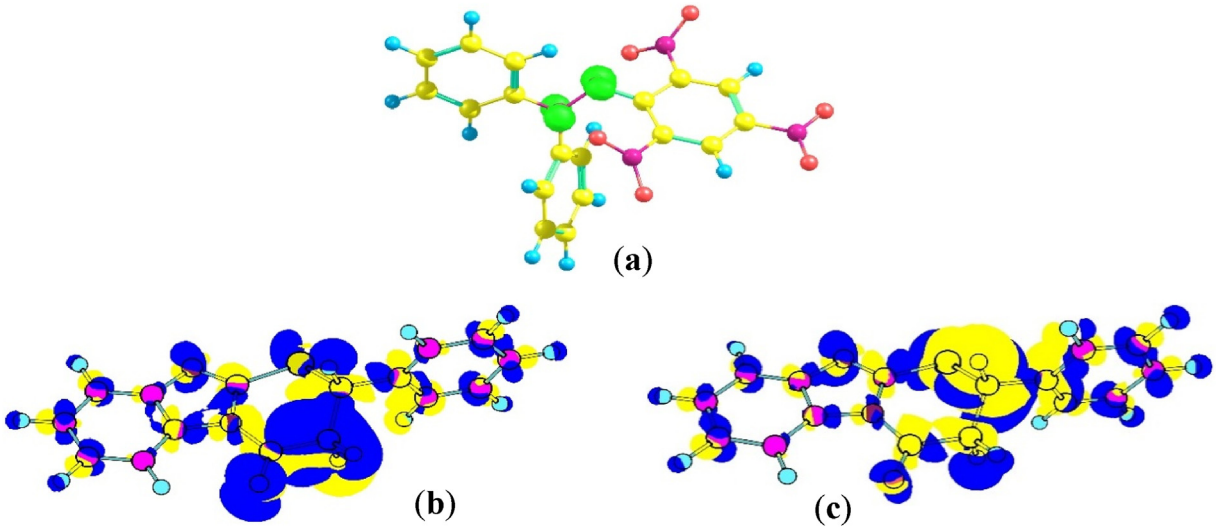

Fig. 12. Spin density plot of the DPPH• optimized structure (**a**) and H function (**b** and **c**) for **III**. In (**b**) and (**c**) the two possible hydrogen transfer mechanisms are shown.

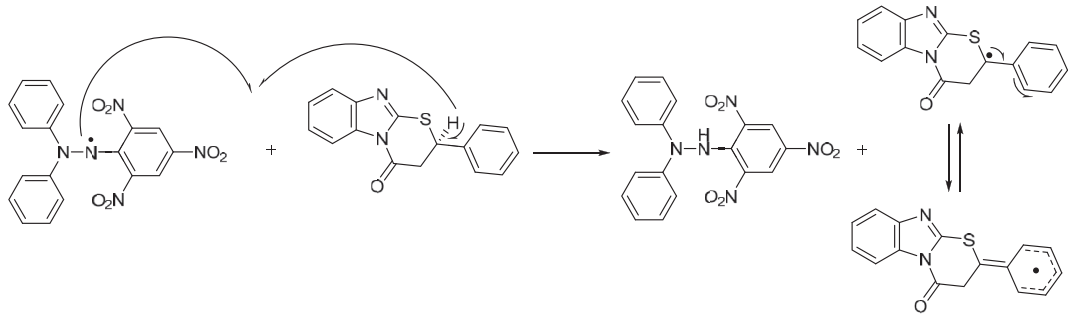

Scheme 2. Possible mechanism of the antioxidant activity of compound **III** in the DPPH• method.

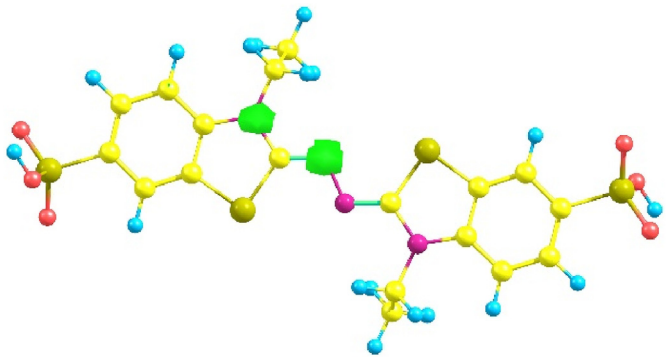

Fig. 13. Spin density plot of the $ABTS^{\bullet+}$ optimized structure.

In order to explain the antioxidant mechanism two sites in the 2-aril-2,3-dihidro-4H- [1,3] thiazino [3,2-a]benzimidazol-4-one system were proposed where hydrogen transfer can be carried out (Fig. 9).

In either case, there is a homolytic cleavage of the C—H bond, where the hydrogen is transferred to the DPPH• radical and now the donating molecule becomes the new radical. Evidently, one of the mechanism proposed is mostly favored. With the purpose to understand, which mechanism is the most viable the reaction coordinate of **a** and **b** was determined at a level B3LYP/D3BJ/6-311G(d,p) (Figs. 10 and 11). It was observed that the two reactions were endothermic and satisfy the Hammond postulate with "product-like" TS [37].

According to the values of TS (96.631 and 42.414 kcal/mol for the site of dehydrogenation **a** and **b** respectively) the most favored mechanism occurs in site **b**. On the other hand, Fig. 12 shows the spin density of the radical DPPH•, as can be seen the favored areas where the electron disappeared is located resides in nitrogen of the radical molecule, this supports the idea that the hydrogen transfer of 2-aryl-2,3-dihydro-4H- [1,3]thiazino [3,2-a]benzimidazole-4-one is oriented towards that area of DPPH•.

The possible mechanism of the antioxidant activity of **III** is shown in Scheme 2 in where the hydrogen of position 12 is transferred to stabilize the radical and form $DPPH_2$. The conjugation of the charge can occur between the C12 of the thiazine ring and the aromatic ring.

Recently, Pineda-Urbina et al., proposed a tool called H function, which allows observation of electron density rearrangement after the extraction of proton, in this study dehydrogenation was analyzed. The results are presented in graphic form as isosurfaces, where decrements in electron density are colored yellow and increments in electron density are colored blue [38].

In order to determine the electron density reorganization in the antioxidant molecule, how a stability measure, the H function was

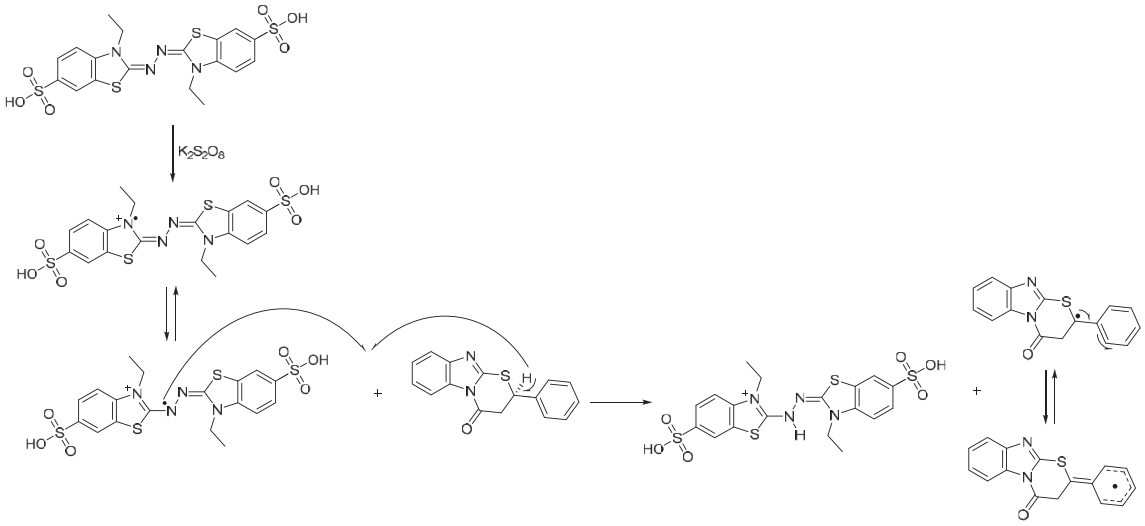

Scheme 3. Possible mechanism of the antioxidant activity of compound **III** in the ABTS$^{\bullet+}$ method.

determined (Fig. 12). The calculation was done for the two possible dehydrogenation sites. In the case of **a** (Fig. 9) it was observed that there is an increase in the electron density in the carbonyl zone, while for **b** (Fig. 9) the implicated zones correspond to the sulphur atom and the benzene ring. The possible resonant structures (Scheme 2) are superior to comparison of **a**, where there is only resonance between C11 and carbonyl, this supports the idea of the favored reaction mechanism (Fig. 10).

3.4.2. ABTS$^{\bullet+}$ method

The percentage of inhibition in ABTS$^{\bullet+}$ method was calculated in the same way as for the DPPH$^{\bullet}$ assay. Compound **III** presented an inhibition of 99% ± 1.18 which compared to the reference antioxidant ascorbic acid (98% ± 0.34) indicates a high scavenging capacity of the ABTS$^{\bullet+}$, also presenting values of 30 mg AAE/L.

In the Fig. 13 shows the spin density of the radical ABTS$^{\bullet+}$, as can be seen the favored areas where the electron disappeared is located resides in nitrogen of the radical molecule, this supports the idea that the hydrogen transfer of compound **III** is oriented towards that area of ABTS$^{\bullet+}$.

According to the reaction conditions for the formation of radical cation, ABTS in its protoned (neutral) form was oxidized by potassium persulphate, where there is the loss of a nitrogen electron (Fig. 13) forming ABTS$^{\bullet+}$. The possible mechanism of the antioxidant activity of **III** versus ABTS$^{\bullet+}$ is shown in Scheme 3, which is similar to that proposed for the DPPH$^{\bullet}$ method.

4. Conclusions

The 2-aryl-2,3-dihydro-4H- [1,3]thiazino [3,2-a]benzimidazol-4-one (**III**) has been synthesized and characterized by ^{1}H NMR, ^{13}C NMR and mono-crystal X-ray diffraction. The compound crystallized in a monoclinic crystal system with $P2_{1/C}$ space group. The thiazine ring is formed by 6 members that have angular tension in the carbon (C12). The compound **III** has three non-covalent intramolecular interactions (C4···N3); (C12···O1); (C11···C7) and (C11···C8) where C11 is a bifurcated donor. In addition, there are interactions π-π between imidazole and benzene ring where the dimerization of the compound extends along the b axis. The major contribution to the total Hirshfeld surfaces was of the (H···H) interactions. These interactions contribute to stabilization of the crystal packing. The result of the antioxidant activity of compound III showed percentage inhibition values like those shown by the reference antioxidants, indicating good anti-radical activity. The antioxidant mechanism for DPPH$^{\bullet}$ and ABTS$^{\bullet+}$ is through HAT (H12) where the conjugation of the charge can occur between the C12 of the thiazine ring and the aromatic ring.

Acknowledgments

Students O.A.R.R. and J.P.M.S thanks CONACYT for a PhD scholarship 330102 and 330098, respectively. A. Cruz thanks CONACYT, México and Secretaría de Investigación y Posgrado-IPN (SIP-IPN) for financial support, Grant 20180754. On the other hand to COTEBAL-IPN and Facultad de Ciencias Químicas de la Universidad de Colima for the facilities given (sabbatical studying 2018–2019).

Appendix F. Supplementary data

Supplementary data to this article can be found online at https://doi.org/10.1016/j.molstruc.2019.127036.

References

[1] K. Mayura, S. Charan, Benzimidazole: an important biological heterocyclic Scaffold, J. Curr. Pharm. Res. 4 (2014) 1159–1167.
[2] A. Rivera, A. Mejia-Camacho, J. Ríos-Motta, M. Dušek, K. Fejfarová, 1,3-Bis(ethoxy-meth-yl)-1H-benzimidazole-2(3H)-thione, J. Acta Crystallogr. E 66 (2010) 1135–1136. https://doi.org/10.1107/S1600536810013036.
[3] J.T. Miller, E.M. Turner, K.S. Gudmundsson, S. Jenkinson, A. Spaltenstein, M. Thomson, P. Wheelan, Novel N-substituted benzimidazole CXCR4 antagonists as potential anti-HIV agents, Bioorg. Med. Chem. Lett 20 (2010) 2125–2128. https://doi.org/10.1016/j.bmcl.2010.02.053.
[4] J. Cheng, J. Xie, X. Luo, Synthesis and antiviral activity against Coxsackie virus B3 of some novel benzimidazole derivatives, Bioorg. Med. Chem. Lett 15 (2005) 267–269. https://doi.org/10.1016/j.bmcl.2004.10.087.
[5] V.N. Britsun, M.O. Lozinskii, Synthesis of 2-Aryl-2,3-dihydro-4H-[1,3]thiazino [3,2-a]benzimidazol-4-ones and 7-Aryl-2,3,6,7-tetrahydro-5H-imidazo[2,1-b]-1,3-thiazin-5-ones, Chem. Heterocycl. Comp. 39 (2003) 960–964.
[6] S. Datta, P. Sambhaji, D. Balasaheb, Synthesis and antioxidant activity of 6-imino-4-(methylthio)-2-(pyridine-3-yl)-6h-1,3-thiazine-5-carbonitrile, Int. Res. J. Pharm. 8 (2017) 160–164. https://doi.org/10.7897/2230-8407.089172.
[7] Y. Özkay, Y. Tunal, H. Karaca, L. Iskdag, Y. Özkay, Y. Tunalı, H. Karaca, İ. Işıkdağ, Antimicrobial activity of a new series of benzimidazole derivatives, J. Arch Pharm. Res. 34 (2011) 1427–1435 (2011), https://doi.org/10.1007/s12272-011-0903-8.
[8] S.K. Doifode, M.P. Wadekar, S. Rewatkar, Synthesis of 1,3-thiazines from

aurones, Orient. J. Chem. 27 (2011) 1265–1267.
[9] T. Sindhu, C. Meena, K. Krishnakumar, Synthesis, characterization and antifungal potential evaluation of 1,4 thiazine derivatives by mannich bases, Hygeia J. Drugs Med. 10 (2018) 27–39. https://doi.org/10.15254/H.J.D.Med.10.2018.175.
[10] V. Sundari, R. Valliappan, Synthesis and biological screening of some thiazine Substituted benzimidazoles, Indian J. Heterocycl. Chem. 14 (2004) 47–50.
[11] S. Gupta, N. Ajmera, P. Meena, N. Guutam, A. Kumar, D. Guatam, Synthesis and biological evaluation of new 1,4-thiazine containing heterocyclic compounds, Jordan, J. Chem. 4 (2009) 209–221.
[12] W. Nawrocka, M. Zimecki, T. Kuznicki, M.W. Kowalska, Immunotropic properties of 2-aminobenzimidazole derivatives in cultures of human peripheral blood cells, part 5, Arch. Pharm. Pharm. Med. Chem. 332 (1999) 85–90. https://doi.org/10.1002/(SICI)1521-4184(19993)332:3%3C85::AID-ARDP85%3E3.0.CO;2-S.
[13] D.W. Wen, C.C. Li, H. Di, Y.P. Liao, H.W. Liu, A universal HPLC method for the determination of phenolic acids in compound herbal medicines, J. Agric. Food Chem. 53 (2005) 6624–6629. https://doi.org/10.1021/jf0511291.
[14] A. Floegel, D.O. Kim, S.J. Chung, S.I. Koo, O.K. Chun, Comparison of ABTS/DPPH assays to measure antioxidant capacity in popular antioxidant-rich US foods, J. Food Compos. Anal. 24 (2011) 1043–1048. https://doi.org/10.1016/j.jfca.2011.01.008.
[15] M.A. Spackman, D. Jayatilaka, Hirshfeld surface analysis, CrystEngComm 11 (2009) 19–32. https://doi.org/10.1039/b818330a.
[16] C.F. Matta, J.H. Trujillo, T.H. Tang, R.F. Bader, Hydrogen-hydrogen bonding: a stabilizing interaction in molecules and crystals, Chem. Eur J. 9 (2003) 1940–1951. https://doi.org/10.1002/chem.200204626.
[17] A.D. Martin, J. Britton, T.L. Easun, A.J. Blake, W. Lewis, M. Schröder, Hirshfeld surface investigation of structure-directing interactions within dipicolinic acid derivatives, Cryst. Growth Des. 15 (2015) 1697–1706. https://doi.org/10.1021/cg5016934.
[18] D.B.G. Williams, M. Lawton, Drying of organic solvents: quantitative evaluation of the efficiency of several desiccants, J. Org. Chem. 75 (2010) 8351–8354. https://doi.org/10.1021/jo101589h.
[19] Bruker, APEX2 (Version 2012.10-0), SAINT (Version 8.27B), SADABS (Version 2012/1), BrukerAXS Inc, Madison, Wisconsin, USA, 2012.
[20] L.J. Farrugia, WinGX and ORTEP for windows: an update, J. Appl. Crystallogr. 45 (2012) 849–854. https://doi.org/10.1107/S0021889812029111.
[21] G.M. Sheldrick, A short history of SHELX, Acta Crystallogr. A. 64 (2008) 112–122. https://doi.org/10.1107/S0108767307043930.
[22] C.F. Macrae, I.J. Bruno, J.A. Chisholm, P.R. Edgington, P. McCabe, E. Pidcock, L. Rodriguez-Monge, R. Taylor, J. van de Streek, P.A. Wood, Mercury CSD 2.0 - new features for the visualization and investigation of crystal structures, J. Appl. Crystallogr. 41 (2008) 466–470. http://doi.org/10.1107/S0021889807067908.
[23] D. O Kim, K.W. Lee, H.J. Lee, C.Y. Lee, Vitamin C equivalent antioxidant capacity (VCEAC) of phenolic phytochemicals, J. Agric. Food Chem. 50 (2002) 3713–3717. https://doi.org/10.1021/jf020071c.
[24] R. Re, N. Pellegrini, A. Proteggente, A. Pannala, M. Yang, C. Rice-Evans, Antioxidant activity applying an improved ABTS radical cation decolorization assay, Free Radic. Biol. Med. 26 (1999) 1231–1237. https://doi.org/10.1016/S0891-5849(98)00315-3.
[25] M.T. Sumaya-Martínez, S. Cruz-Jaime, E. Madrigal-Santillán, J.D. García-Paredes, R. Cariño-Cortés, N. Cruz-Cansino, C. Valadez-Vega, L. Martinez-Cardenas, E. Alanís-García, Betalain, acid ascorbic, phenolic contents and antioxidant properties of purple, red, yellow and white cactus pears, Int. J. Mol. Sci. 12 (2011) 6452–6468. https://doi.org/10.3390/ijms12106452.
[26] M.J. Frisch, G.W. Trucks, H.B. Schlegel, G.E. Scuseria, M.A. Robb, J.R. Cheeseman, G. Scalmani, V. Barone, B. Mennucci, G.A. Petersson, H. Nakatsuji, M. Caricato, X. Li, H.P. Hratchian, A.F. Izmaylov, J. Bloino, G. Zheng, J.L. Sonnenberg, M. Hada, M. Ehara, K. Toyota, R. Fukuda, J. Hasegawa, M. Ishida, T. Nakajima, Y. Honda, O. Kitao, H. Nakai, T. Vreven, J.A. Montgomery Jr., J.E. Peralta, F. Ogliaro, M. Bearpark, J.J. Heyd, E. Brothers, K.N. Kudin, V.N. Staroverov, R. Kobayashi, J. Normand, K. Raghavachari, A. Rendell, J.C. Burant, S.S. Iyengar, J. Tomasi, M. Cossi, N. Rega, J.M. Millam, M. Klene, J.E. Knox, J.B. Cross, V. Bakken, C. Adamo, J. Jaramillo, R. Gomperts, R.E. Stratmann, O. Yazyev, A.J. Austin, R. Cammi, C. Pomelli, J.W. Ochterski, R.L. Martin, K. Morokuma, V.G. Zakrzewski, G.A. Voth, P. Salvador, J.J. Dannenberg, S. Dapprich, A.D. Daniels, Ö. Farkas, J.B. Foresman, J.V. Ortiz, J. Cioslowski, D.J. Fox, Gaussian 09, Revision E.01, Gaussian, Inc., Wallingford CT, 2009.
[27] A.D. Becke, Density-functional thermochemistry. III. The role of exact exchange, J. Chem. Phys. 98 (1993) 5648–5652. https://doi.org/10.1063/1.464913.
[28] O. Vázquez-Vuelvas, J. Hernández-Madrigal, R. Gaviño, M. Tlenkopatchev, D. Morales-Morales, J. Germán-Acacio, A. Pineda-Contreras, X.- ray, DFT, FTIR and NMR structural study of 2, 3-dihydro-2-(R-phenylacylidene)-1, 3, 3-trimethyl-1H-indole, J. Mol. Struct. 987 (2011) 106–118. https://doi.org/10.1016/j.molstruc.2010.12.001.
[29] T. Lu, F. Chen, Multiwfn: a multifunctional wavefunction analyzer, J. Comput. Chem. 33 (2012) 580–592.
[30] W. Humphrey, A. Dalke, K. Schulten, VMD: visual molecular dynamics, J. Mol. Graph. 14 (1996) 33–38.
[31] S. Grimme, S. Ehrlich, L. Goerigk, Effect of the damping function in dispersion corrected density functional theory, J. Comput. Chem. 32 (2011) 1456–1465. https://doi.org/10.1002/jcc.21759.
[32] S.K. Wolff, D.J. Grimwood, J.J. McKinnon, M.J. Turner, D. Jayatilaka, M.A. Spackman, Crystal Explorer Ver. 3.1, University of Western Australia, Perth, Australia, 2013.
[33] R. Soman, S. Sujatha, C. Arunkumar, Quantitative crystal structure analysis of fluorinated porphyrins, J. Fluorine Chem. 163 (2014) 16–22. https://doi.org/10.1016/j.jfluchem.2014.04.002.
[34] E.R. Johnson, S. Keinan, P. Mori-Sánchez, J. Contreras-García, A.J. Cohen, W. Yang, Revealing noncovalent interactions, J. Am. Chem. Soc. 132 (2010) 6498–6506. https://doi.org/10.1021/ja100936w.
[35] J.M. Berger, R.J. Rana, H. Javeed, I. Javeed, S.L. Schulien, Radical quenching of 1,1-diphenyl-2-picrylhydrazyl: a spectrometric determination of antioxidant behavior, J. Chem. Educ. 85 (2008) 408–410. https://doi.org/10.1021/ed085p408.
[36] R.L. Prior, X. Wu, K. Schaich, Standardized methods for the determination of antioxidant capacity and phenolics in foods and dietary supplements, J. Agric. Food Chem. 53 (2005) 4290–4302. https://doi.org/10.1021/jf0502698.
[37] G.S. Hammond, A correlation of reaction rates, J. Am. Chem. Soc. 77 (1955) 334–338.
[38] K. Pineda-Urbina, Z. Gómez-Sandoval, R. Flores-Moreno, h function: a protonic take on the numerical Fukui function as a graphical descriptor for deprotonation, Int. J. Quantum Chem. 118 (2018), e25532. https://doi.org/10.1002/qua.25532.